Applied Energy 99 (2012) 324–333

Contents lists available at SciVerse ScienceDirect

Applied Energy

journal homepage: www.elsevier.com/locate/apenergy

Performance analysis of four modified approaches for wind speed forecasting

Wenyu Zhang [a,b], Jie Wu [c,*], Jianzhou Wang [c], Weigang Zhao [c], Lin Shen [c]

[a] Key Laboratory for Semi-Arid Climate Change of the Ministry of Education, College of Atmospheric Sciences, Lanzhou University, Lanzhou 730000, China
[b] Key Laboratory of Arid Climatic Change and Reducing Disaster of Gansu Province, Lanzhou 730000, China
[c] School of Mathematics & Statistics, Lanzhou University, Lanzhou 730000, China

HIGHLIGHTS

- Seasonal compact to wind speed forecasting is taken into account.
- Multiple criterions are used as measures for evaluating forecasting quality.
- We examine superiority of the modified models in different wind observation sites.
- All of the modified models are more accurate than the original methods.

ARTICLE INFO

Article history:
Received 25 October 2011
Received in revised form 24 May 2012
Accepted 25 May 2012
Available online 23 June 2012

Keywords:
Wind speed forecasting
Parameter selection
Data decomposition
Evaluation criterion

ABSTRACT

Providing accurate wind speed prediction algorithms has become increasingly significant because of the important technological and economic impacts of wind speed on wind power generation. In this study, two combined strategies for wind speed forecasting are proposed and followed. Four approaches derived from these strategies are employed. The first two approaches employ Particle Swarm Optimization (PSO) to optimize the parameters in the first-order and second-order adaptive coefficient (FAC and SAC) methods. The remaining two approaches employ the decomposition of wind speed data into seasonal and trend components. The seasonal component is represented by the seasonal exponential adjustment, and the trend component is predicted by the hybrid models of PSO and FAC or SAC. By employing these four approaches, the daily mean wind speed is forecasted for four observation sites in Gansu, China. Multiple evaluation methods are used to assess forecasting quality: the mean square error, the mean absolute percentage error and the relative error. It is found that all four approaches better predict wind speed than the original FAC and SAC models.

1. Introduction

Because of increasing energy consumption, the limited reserves of fossil fuels and conventional fuels will no longer meet the growing demand. Meanwhile, more attention has being drawn to the adverse environmental effects caused by traditional fossil fuels. As a consequence, it is imperative and advisable to seek sustainable, clean and environmentally friendly alternative energy resources. Because wind power is a pollution-free and sustainable energy that does not contribute to global warming, it is often regarded as a potential replacement for fossil fuels. The implementation of wind power in electric power systems is growing rapidly. As indicated in [1], wind power systems have been playing a vital role in everyday life for people in developing countries who live without electricity and who account for one-third of the world's total population. For developed countries, as one source of renewable energy, wind energy will greatly support them to fulfill the plan of meeting the energy consumption demand during the 21st century. A conservative estimate indicates that the global wind power potential is approximately 20,000 TW h/year [2]; once this potential can be fully utilized, wind power will make an enormous contribution to the balance of the world's energy.

However, in the practical application of wind power, a problem is that electricity from wind energy cannot be as steadily generated as electricity from other sources due to the uncertainty in the generated amount and intermittency of wind power. Factors such as wind speed, air density and turbine characteristics will all cause variations of the wind energy produced. Specifically, the amount of wind energy produced varies with the cube of the wind speed. Therefore, it is imperative that the accuracy of wind speed prediction be improved to attain more accurate predictions of wind power generation.

Recently, many models have been suggested to improve the accuracy of wind speed prediction, such as conventional statistical models [3,4], neural networks [5], fuzzy logic [6], support vector

* Corresponding author. Tel.: +86 931 8914050; fax: +86 931 8912481.
E-mail address: wuj19870903@126.com (J. Wu).

0306-2619/$ - see front matter © 2012 Elsevier Ltd. All rights reserved.
http://dx.doi.org/10.1016/j.apenergy.2012.05.029

machine [7] and spatial–temporal models [8]. In addition, applying hybrid models based on these approaches to modeling wind speed are frequently used. For instance, Monfared et al. [9] designed a strategy which uses hybrid methods of neural networks and fuzzy logic. With actual wind speed time series sampled in Rostamabad from 2002 to 2005, these authors showed that this approach both requires less computational time and provides better prediction performance. A hybrid method which consists of artificial neural networks and Bayesian methods was proposed by Li et al. [10]. The results indicated that, in contrast to artificial neural networks, whose performance is not consistent when the site or evaluation criterion changes, prediction errors presented by the Bayesian combination approach always become smaller. Cadenas and Rivera [11] developed hybrid methods which consist of Artificial Neural Network (ANN) and Autoregressive Integrated Moving Average (ARIMA). The authors concluded that the combined models outperform the individual ANN and ARIMA approaches. To predict wind speed in the short-term, Sancho et al. [12] developed the hybridization of artificial neural networks with the mesoscale model. They found that this combination strategy was successful and was superior in its forecasting results.

Parameter and input data selection also have a great impact on the wind speed forecasting accuracy of models; thus, work has been performed related to the strategy thereof. ARIMA models are frequently employed to predict wind speed where the differencing parameter '*d*' is always set to an integer. Uniquely, Rajesh and Krithika [13] studied an ARIMA model named fractional-ARIMA where the differencing parameter '*d*' was assumed to be a fractional number. It was found that the proposed models give better forecasting results compared with the persistence method. Fan and Liu [14] made a revised parameter based on the weighted forecasting method of Gray related degree. The effectiveness of the proposed model was demonstrated using a test in a certain area. In addition to the Evolutionary Programming method, Particle Swarm Optimization was also used to estimate the hyper-parameters in Support Vector Machines regressions by Sancho et al. [15]. The complete evolutionary approach was then adopted for wind speed forecasting at a wind farm in Spain and experiment showed that this algorithm was superior to a previous model which used a multi-layer perceptron in the regression process. Colorado et al. [16] developed a methodology according to the laws of thermodynamics and inverse neural networks with the purpose of reducing the irreversibility of the heat transformer. This modified methodology was quite useful for calculating the most suitable input parameters to ensure lower irreversibilities in the heat transformer operation. Additionally, Louka et al. [17] published an application of using filtered data as the input for wind energy forecasting. The results showed that this idea really supplied valid forecasting for long horizons. For neural networks, Sancho et al. [18] exploited diversity in the input data to prove that this method obtained preferable results to those from a single artificial neural network.

The above models all reconstructed the wind speed time series from previous data. Some techniques have also been designed to include other geographical and atmospheric variables such as altitude, wind direction, local temperature, radiation or pressure at the measuring point. For example, latitude, longitude, altitude and month were adopted by Fadare [19] as elements in the input layer of the ANN network, while the data in the output layer was set as the monthly average wind speed. An acceptable accuracy was obtained in this study.

These and other studies all come to a similar conclusion that accurate wind speed forecasting is particularly important. To reduce the forecasting error, more modified forecasting models need to be developed. Taking into account the fact that hybrid algorithms combined with other algorithms and parameter selection can always improve the forecasting accuracy, this paper concentrates on obtaining satisfactory forecasting results using both of these ideas. PSO is a useful tool in selecting the most suitable parameter; therefore, it is applied in this study to improve the forecasting accuracy. In addition, the seasonal and trend components coexist in wind speed data in general. Thus, the seasonal exponential adjustment technique is first employed to guarantee that the primary data series is free from the influence of the seasonal trend, and then the trend component is forecasted separately. Based on these ideas, two combined strategies and four modified forecasting models based on first-order adaptive coefficient (FAC) and second-order adaptive coefficient (SAC) methods are proposed. Then, the performances of these models are evaluated using the actual wind speed data sampled from four observation sites in Gansu and three error evaluation criteria, namely the mean square error, the mean absolute percentage error and the relative error.

The remainder of this paper is organized as follows. Related methodologies are briefly described in Section 2. In Section 3, two combined strategies and four modified models based on FAC and SAC are proposed. Simulation and model evaluation results are reported in the fourth section. Finally, Section 4 presents conclusions from the study.

2. Related algorithms

In this section, the conventional FAC and SAC models are introduced first. We then furnish a brief introduction of the seasonal exponential adjustment (SEA) technique. Lastly, the parameter selection approach—PSO—is described.

2.1. Conventional FAC and SAC approach

FAC and SAC are two adaptive forecasting models in which their parameters are updated continuously so that the models are more flexible.

2.1.1. FAC method

As a common prediction strategy, employing the weighted average of the latest data x_t ($t \leqslant T$) and the historical forecasted value $\hat{x}_t$ to obtain the value of the next moment $\widehat{x}_{t+1}$ is frequently applied. That is,

$$\hat{x}_{t+1} = \alpha x_t + (1-\alpha)\hat{x}_t. \tag{1}$$

However, in general, one fixed α is not suitable for every occasion. Therefore, by replacing α with α_t, which varies with t, we write formula (1) as

$$\hat{x}_{t+1} = \alpha_t x_t + (1-\alpha_t)\hat{x}_t \tag{2}$$

or

$$\hat{x}_{t+1} = \hat{x}_t + \alpha_t(x_t - \hat{x}_t) = \hat{x}_t + \alpha_t e_t, \tag{3}$$

where $e_t = x_t - \widehat{x}_t$ is the residual error.

The FAC method is proposed based on this idea, where α_t is determined through a novel approach. In this method, determination strategies of α_t are different depending on the sign of e_t. Generally, the situation is divided into two categories:

a. A systematic error exists; therefore, all values of e_t are either positive or negative. In this case, α_t should be adjusted according to the rules shown in Fig. 1.
b. No systematic error exists. In this situation, values of e_t appear alternately positive and negative, and $|e_t|$ is not too large, so α_t can remain unchanged.

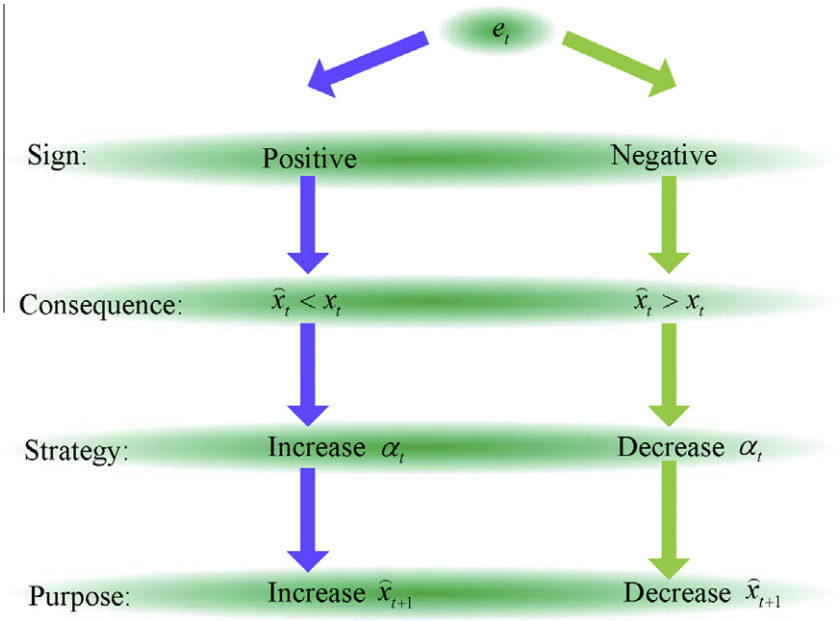

Fig. 1. Rules adopted in adjusting α_t when the systematic error exists.

The systematic error can be measured as follows:

Assign a value to $\beta(0 < \beta < 1)$ and a weight to each e_k $(k = 1,2,\ldots,t)$, then the systematic error can be calculated via $|E_t|$, where E_t is defined as

$$E_t = \beta e_t + \beta(1-\beta)e_{t-1} + \cdots + \beta(1-\beta)^{t-1}e_1. \quad (4)$$

Similarly, another variable M_t is defined as

$$M_t = \beta|e_t| + \beta(1-\beta)|e_{t-1}| + \cdots + \beta(1-\beta)^{t-1}|e_1|. \quad (5)$$

Then, the adaptive coefficient is calculated by the FAC method using

$$\alpha_t = |E_t|/M_t. \quad (6)$$

Thus, α_t always varies between 0 and 1.

2.1.2. SAC method

Because low order algorithms do not always satisfy the forecasting accuracy demand, a higher order algorithm should be introduced. The SAC model proposed is based on the FAC. Two additional variables are introduced, $S_t^{(1)}$ and $S_t^{(2)}$, which are defined as

$$S_t^{(1)} = \alpha_t x_t + (1-\alpha_t)S_{t-1}^{(1)}, \quad (7)$$

$$S_t^{(2)} = \alpha_t S_t^{(1)} + (1-\alpha_t)S_{t-1}^{(2)}, \quad (8)$$

where $S_0^{(1)} = S_0^{(2)} = x_1$. The SAC approach then defines the forecasted value $\hat{x}_{t+1}$ as follows:

$$\hat{x}_{t+1} = \hat{a}_t + \hat{b}_t, \quad (9)$$

where

$$\hat{a}_t = 2S_t^{(1)} - S_t^{(2)} \quad (10)$$

and

$$\hat{b}_t = \frac{\alpha_t}{1-\alpha_t}\left[S_t^{(1)} - S_t^{(2)}\right]. \quad (11)$$

Flowcharts of FAC and SAC are plotted in Fig. 2.

Generally, the value of β in FAC or SAC is set to 0.2.

2.2. Seasonal exponential adjustment (SEA)

Generally, the trend and seasonal components exist in the same wind speed dataset. Actually, the wind speed at time s can be expressed as [20]

$$x_s = \textit{Trend component} \times \textit{Seasonal component}. \quad (12)$$

Then, the seasonal index is given by

$$I_s = x_s/\textit{Trend component}. \quad (13)$$

Because the trend component was unknown, the average of x_i in each cycle was often used as its approximation.

Rearranging the dataset $x_1,x_2,\ldots,x_T$ to be $x_{11},x_{12},\ldots,x_{1l};\ldots;$ $x_{k1},x_{k2},\ldots,x_{kl};\ldots;$ and $x_{m1},x_{m2},\ldots,x_{ml}(k = 1,2,\ldots,m;\ s = 1,2,\ldots,l,$ $T = m \times l)$, where m represents the number of cycles and in each cycle, there are l data items, the seasonal index I_s can be obtained by the process shown in Fig. 3.

Finally, by rearranging the data items $x'_{11},x'_{12},\ldots,x'_{1l};\ldots;$ $x'_{m1},x'_{m2},\ldots,x'_{ml}$ back to $x'_1,x'_2,\ldots,x'_T$, datasets without the effect of that seasonal trend can be obtained.

2.3. Particle Swarm Optimization (PSO)

For the last several decades, studies have actively focused on the evolution of the models from the perspective of algorithm combination and parameter selection. As one parameter selection approach, PSO is employed to solve many dynamic problems.

All of the solutions, called "particles", in the PSO algorithm are assessed by the objective function and are directed by the velocities to find a better position [21]. In the process of updating particles, two "best" values are used: p_{best} and g_{best}, which represent the best position of the specific particle and that of all particles, respectively. The single particle's position and velocity are updated by Eqs. (14) and (15):

$$v_i(t+1) = \omega \cdot v_i(t) + c_1 \cdot ud_{ij} \cdot [p_i(t) - x_i(t)] + c_2 \cdot Ud_{ij} \cdot [p_g(t) - x_i(t)] \quad (14)$$

$$x_i(t+1) = x_i(t) + v_i(t+1) \quad (15)$$

where $v_i(t) = (v_{i1}(t), v_{i2}(t),\ldots, v_{ik}(t))$ and $x_i(t) = (x_{i1}(t),x_{i2}(t),\ldots,x_{ik}(t))$. The jth dimension of the ith particle is updated by the current velocity $v_{ij}(t)$ and position $x_{ij}(t)$, and $p_g = (p_{g1},p_{g2},\ldots,p_{gk})$ represents

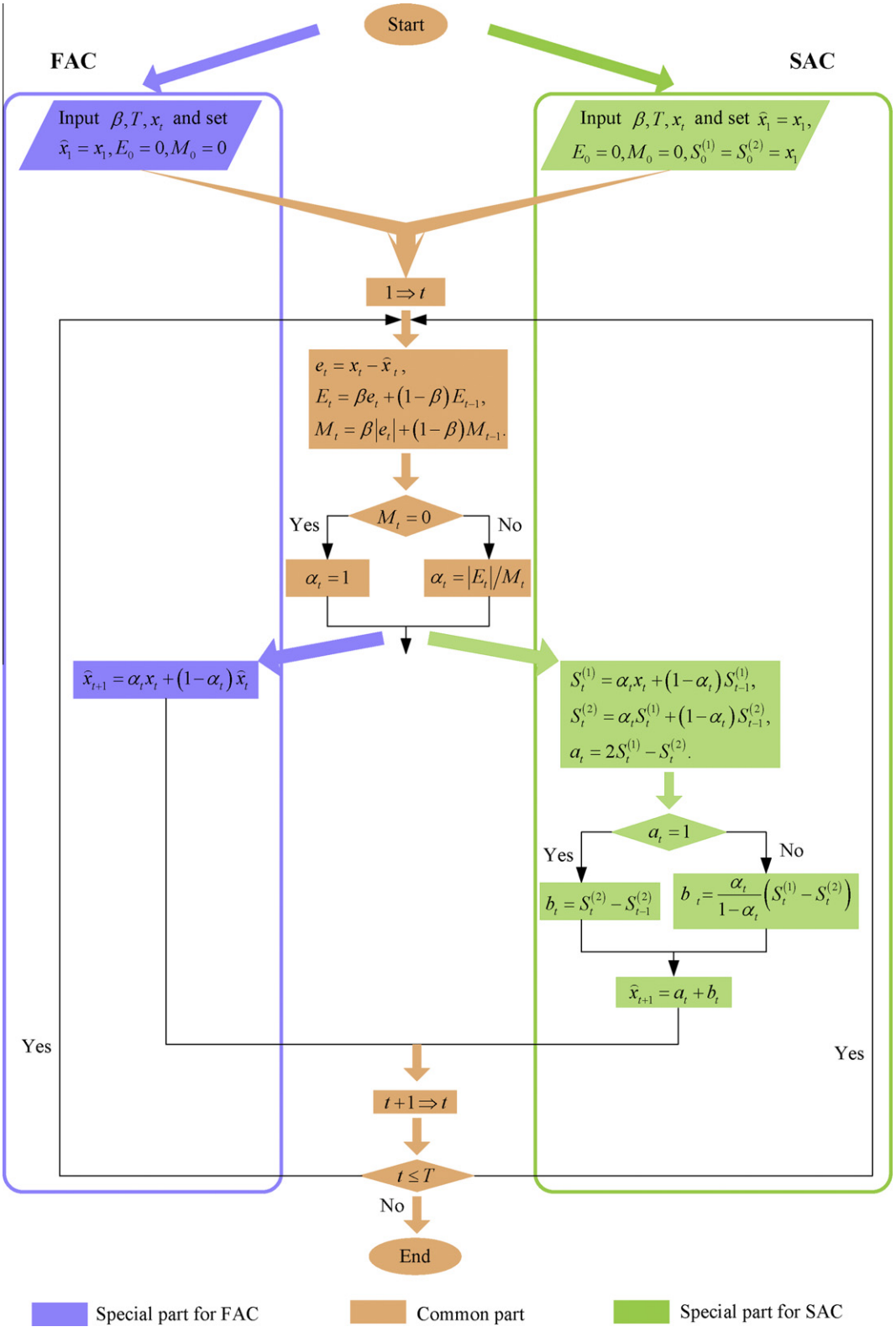

Fig. 2. Flowcharts of FAC and SAC.

the most suitable position among the total particles at present. The cognitive and social constants, denoted as c_1 and c_2, respectively, are both positive and are the acceleration constants responsible for varying the particle velocity towards p_{best} and g_{best} [22]. ud_{ij} and Ud_{ij} are uniform random numbers between 0 and 1.

2.4. Combined strategies and modified models

As mentioned in Section 2.1.2, the value of β in FAC or SAC is usually set to 0.2. However, this value is not always suitable for all situations, and its usage could even produce negative effects.

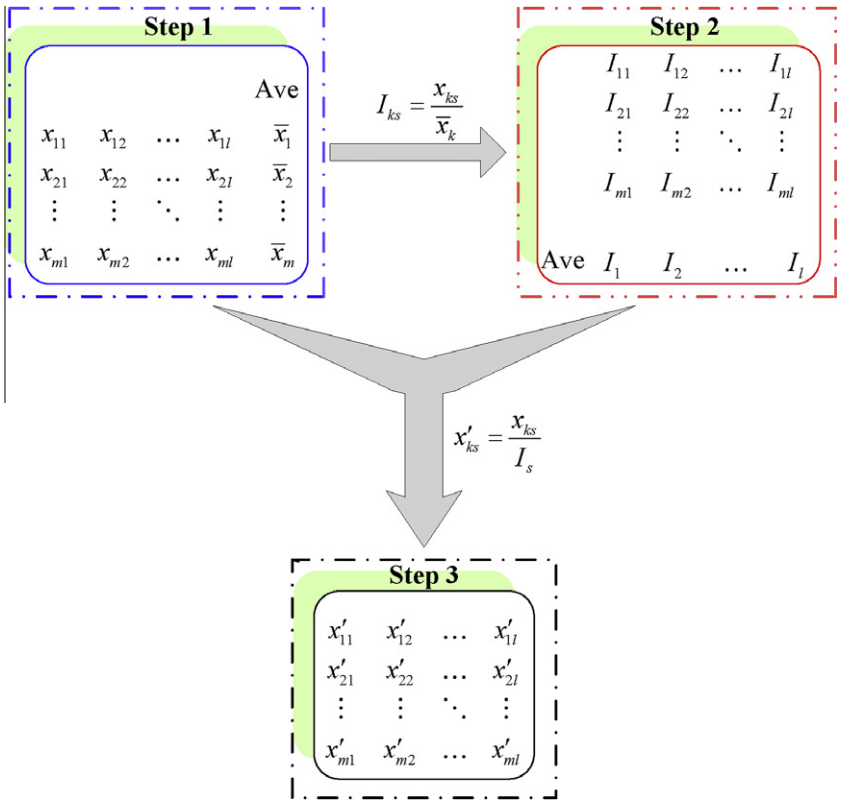

Fig. 3. Calculation process of seasonal index.

Hence, PSO is used to choose the most suitable value for β. Moreover, a seasonal component exists in the wind speed data and is associated with the trend component; therefore, a seasonal exponential adjustment is first implemented to remove the seasonal component from the wind speed time series as an attempt to improve the forecasting accuracy. The flowchart of the proposed hybrid model is shown in Fig. 4.

As shown in Fig. 4, there are two combined strategies:

a. *Combined strategy 1:* Only PSO and either FAC or SAC are combined to predict wind speed and the two modified models are abbreviated as PFAC and PSAC, respectively.
b. *Combined strategy 2:* Before PSO and FAC or SAC are combined, SEA is employed to remove the influence of the seasonal trend from the primary data series. These two modified models are abbreviated as SPFAC and SPSAC.

By introducing these two combined strategies, it can be observed whether parameter selection and data decomposition appreciably contribute to an improvement in wind speed forecasting accuracy.

3. Simulation results

3.1. Data representation

The daily mean wind speed data used for simulation in this paper are sampled from four observation sites in the Hexi Corridor of the Gansu province: Jiuquan, Mazongshan, Wuwei and Zhangye. Their longitudes and altitudes are shown in Table 1, and geographic locations of these four sites are displayed in Fig. 5 [23].

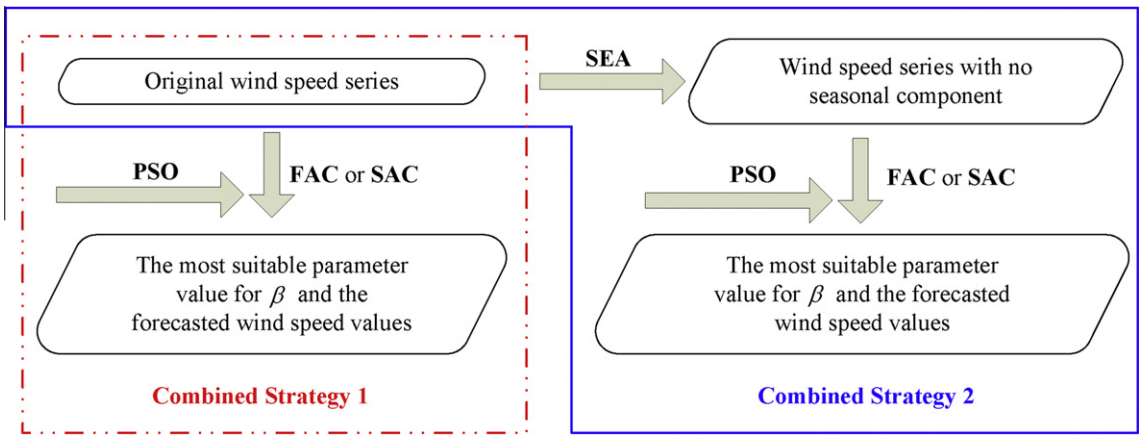

Fig. 4. Flowchart of the two combined strategies.

Table 1
The longitude and altitude of the four observation sites in the Hexi Corridor.

Area	East longitude	North latitude	Highest altitude (m)	Lowest altitude (m)
Jiuquan	98°31′	39°44′	1500	1350
Mazongshan	97°03′	41°8′	2000	1500
Wuwei	37°56′	102°39′	3045	1367
Zhangye	100°26′	38°56′	1700	1200

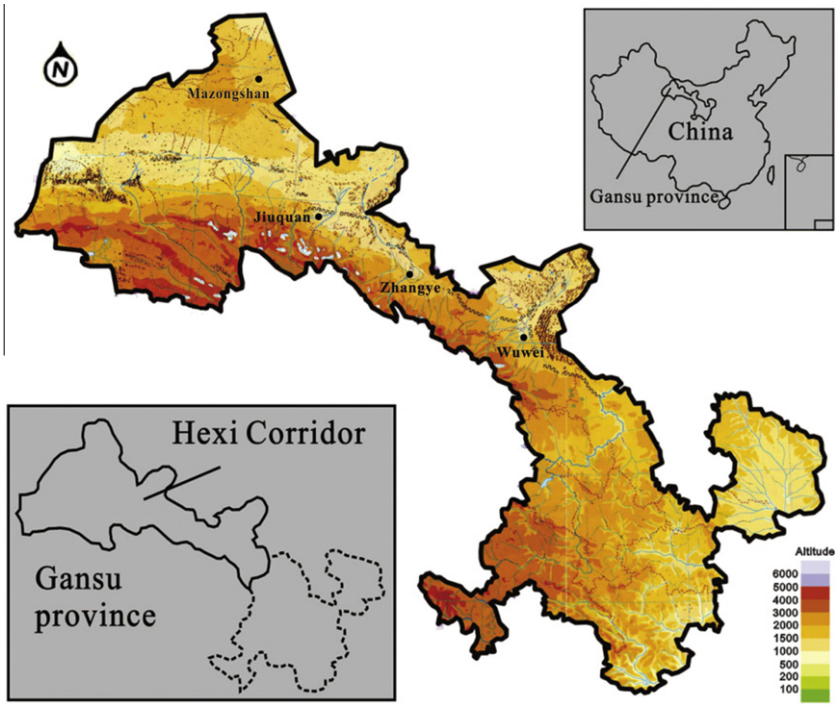

Fig. 5. Topographic map of the four observation sites in the Hexi Corridor.

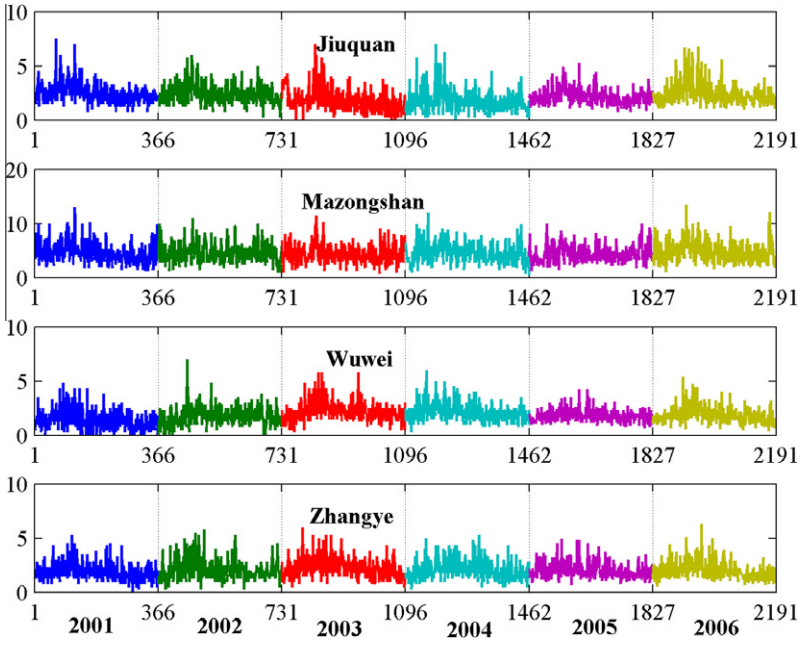

Fig. 6. Wind speed data from the four observation sites.

Table 2
Parameter and error values in 2006 forecasted by six models.

Site	Month	Forecasted results							Month	Forecasted results							Month	Forecasted Results						
			FAC	SAC	PFAC	PSAC	SPFAC	SPSAC			FAC	SAC	PFAC	PSAC	SPFAC	SPSAC			FAC	SAC	PFAC	PSAC	SPFAC	SPSAC
Jiuquan	January	β	0.2000	0.2000	0.0642	0.0275	0.0832	0.0307	February	β	0.2000	0.2000	0.0062	9.6×10^{-18}	5.6×10^{-4}	0.0099	March	β	0.2000	0.2000	6.2×10^{-17}	0.0073	0.8961	0.0075
		MSE	0.5588	0.7516	0.4880	0.5015	0.4880	0.4980		MSE	0.9590	1.2545	0.7525	0.7374	0.5816	0.5854		MSE	1.8530	2.4168	1.3351	1.4053	1.0849	1.0425
		MAPE	25.42	28.72	24.72	22.51	25.91	26.71		MAPE	37.60	40.53	27.76	28.56	28.34	32.85		MAPE	33.55	33.90	31.88	37.79	34.29	39.30
	April	β	0.2000	0.2000	1.5×10^{-17}	3.4×10^{-17}	2.0×10^{-16}	4.8×10^{-17}	May	β	0.2000	0.2000	0.0297	0.0081	0.0302	0.0116	June	β	0.2000	0.2000	3.4×10^{-18}	0.0093	3.8×10^{-17}	8.4×10^{-18}
		MSE	2.2193	2.9110	1.6189	1.5934	1.3433	1.3153		MSE	1.2369	1.6687	1.0522	0.9435	0.8063	0.7501		MSE	0.7998	1.1137	0.5935	0.6002	0.5072	0.5010
		MAPE	50.66	52.49	38.53	35.21	40.95	38.46		MAPE	41.64	45.89	37.62	38.70	38.45	39.81		MAPE	42.86	54.53	29.86	39.57	35.12	33.79
	July	β	0.2000	0.2000	4.1×10^{-17}	3.9×10^{-17}	4.9×10^{-17}	2.0×10^{-19}	August	β	0.2000	0.2000	1.7×10^{-16}	0.0144	0.0436	0.0200	September	β	0.2000	0.2000	0.0204	0.0091	0.0306	0.0159
		MSE	0.7508	1.0190	0.6106	0.6038	0.5975	0.5819		MSE	0.6157	0.7701	0.5229	0.5386	0.5385	0.5319		MSE	0.7410	0.9627	0.5658	0.5761	0.5865	0.6242
		MAPE	37.00	43.44	26.11	22.32	33.00	26.99		MAPE	23.30	27.74	21.05	20.95	22.38	22.28		MAPE	33.79	34.64	24.80	25.80	38.32	37.65
	October	β	0.2000	0.2000	8.3×10^{-18}	0.0099	0.0659	0.0199	November	β	0.2000	0.2000	0.0241	0.0060	0.0206	0.0098	December	β	0.2000	0.2000	4.1×10^{-18}	0.0050	0.0596	0.0274
		MSE	0.5644	0.7974	0.4789	0.4923	0.3714	0.3727		MSE	0.6098	0.8478	0.5192	0.5449	0.4331	0.4536		MSE	0.5208	0.6687	0.4931	0.5121	0.4635	0.4896
		MAPE	17.11	19.08	19.05	21.39	19.92	23.95		MAPE	28.73	32.86	26.35	28.20	25.45	26.85		MAPE	25.67	30.72	24.77	30.01	32.60	32.89
Mazongshan	January	β	0.2000	0.2000	1.6×10^{-17}	0.0053	0.0052	0.0057	February	β	0.2000	0.2000	3.4×10^{-16}	3.4×10^{-17}	0.1086	4.5×10^{-17}	March	β	0.2000	0.2000	0.0018	2.0×10^{-17}	0.0020	2.2×10^{-17}
		MSE	3.8097	4.7812	3.0566	3.3392	2.4130	2.7448		MSE	4.3334	6.1612	3.5042	3.3610	2.9298	2.7032		MSE	3.6317	4.7836	2.9411	2.8213	2.5200	2.4495
		MAPE	41.55	45.37	34.86	35.86	38.17	36.74		MAPE	45.98	50.15	42.17	40.88	48.48	41.32		MAPE	33.06	37.95	26.89	26.25	27.93	27.00
	April	β	0.2000	0.2000	6.0×10^{-16}	2.4×10^{-17}	2.2×10^{-17}	5.4×10^{-17}	May	β	0.2000	0.2000	3.1×10^{-18}	4.3×10^{-17}	0.0035	2.7×10^{-17}	June	β	0.2000	0.2000	0.0028	4.0×10^{-18}	0.0095	7.4×10^{-18}
		MSE	5.1256	6.2444	4.4114	4.2510	3.7212	3.5531		MSE	3.8552	4.3531	3.0710	2.9811	2.5934	2.5746		MSE	3.3368	4.5484	2.3205	2.2371	1.8226	1.7134
		MAPE	35.37	36.10	27.40	24.31	28.20	24.94		MAPE	36.14	35.30	33.93	32.87	34.24	35.60		MAPE	37.97	44.17	31.28	30.28	29.38	31.46
	July	β	0.2000	0.2000	0.0013	3.6×10^{-17}	3.5×10^{-17}	7.4×10^{-18}	August	β	0.2000	0.2000	0.0011	3.9×10^{-17}	0.0018	4.9×10^{-17}	September	β	0.2000	0.2000	0.0043	2.9×10^{-17}	0.0044	4.3×10^{-17}
		MSE	2.6881	3.6719	2.1976	2.1323	2.0248	1.9313		MSE	2.5344	2.9738	2.0247	2.0351	1.8040	1.8101		MSE	2.0952	2.7116	1.5329	1.4578	1.4051	1.3636
		MAPE	42.87	45.95	37.16	35.69	38.02	35.46		MAPE	33.02	38.00	26.90	26.47	26.22	25.44		MAPE	33.69	41.51	31.72	30.04	38.08	35.18
	October	β	0.2000	0.2000	4.0×10^{-16}	3.9×10^{-17}	0.0789	5.3×10^{-17}	November	β	0.2000	0.2000	5.5×10^{-17}	1.1×10^{-17}	1.2×10^{-16}	7.3×10^{-18}	December	β	0.2000	0.2000	2.5×10^{-4}	3.5×10^{-17}	5.6×10^{-4}	0.0334
		MSE	3.1643	3.9717	2.4280	2.3486	2.6179	2.4893		MSE	3.7639	4.4327	3.2474	3.2179	2.6833	2.5864		MSE	4.1623	5.3477	4.0143	4.1340	3.8650	4.5705
		MAPE	30.44	35.97	33.87	33.35	31.96	28.98		MAPE	31.77	38.15	36.20	35.79	31.10	28.02		MAPE	34.44	33.47	45.39	41.33	48.39	44.37
Wuwei	January	β	0.2000	0.2000	3.7×10^{-17}	0.0072	1.5×10^{-17}	0.0079	February	β	0.2000	0.2000	0.0282	0.0087	1.0×10^{-16}	0.0124	March	β	0.2000	0.2000	3.9×10^{-17}	2.1×10^{-17}	2.0×10^{-17}	0.0089
		MSE	0.4611	0.5940	0.3701	0.3750	0.3473	0.3511		MSE	0.7050	0.8903	0.5972	0.5862	0.5431	0.5426		MSE	1.3556	1.9270	0.9517	0.9905	0.8149	0.8490
		MAPE	24.14	26.30	21.70	20.88	22.74	21.37		MAPE	27.42	34.05	22.67	22.83	24.37	23.91		MAPE	32.12	33.46	30.14	32.73	40.10	26.73
	April	β	0.2000	0.2000	4.6×10^{-17}	0.0050	3.3×10^{-17}	0.0092	May	β	0.2000	0.2000	1.4×10^{-17}	0.0065	1.3×10^{-16}	0.0054	June	β	0.2000	0.2000	6.8×10^{-17}	0.0113	4.2×10^{-17}	0.0488
		MSE	1.1996	1.7345	0.9106	0.9330	0.7429	0.7889		MSE	0.9659	1.3003	0.7627	0.8004	0.6923	0.7520		MSE	1.0025	1.2777	0.7256	0.8263	0.7062	0.8142
		MAPE	45.18	52.20	33.43	31.70	32.59	34.58		MAPE	31.58	37.78	28.21	26.65	32.14	31.59		MAPE	34.04	43.11	33.52	34.89	33.63	39.22
	July	β	0.2000	0.2000	0.0325	0.0092	0.0361	0.0154	August	β	0.2000	0.2000	1.7×10^{-16}	0.0106	2.2×10^{-16}	0.0187	September	β	0.2000	0.2000	4.6×10^{-17}	0.0108	0.0473	2.7×10^{-17}
		MSE	0.7042	0.9216	0.5577	0.5736	0.4718	0.4888		MSE	0.7032	0.9651	0.5212	0.5567	0.4654	0.5059		MSE	0.5056	0.6548	0.3738	0.3767	0.3554	0.3462
		MAPE	47.63	53.60	37.92	33.89	35.71	34.35		MAPE	30.49	36.25	26.87	24.52	28.01	30.60		MAPE	39.76	43.71	44.75	34.64	38.09	38.23
	October	β	0.2000	0.2000	0.0689	0.0298	0.0557	0.0216	November	β	0.2000	0.2000	0.0140	0.0060	0.0153	0.0070	December	β	0.2000	0.2000	1.4×10^{-16}	2.0×10^{-17}	2.5×10^{-16}	0.0110
		MSE	0.5377	0.6690	0.4522	0.4498	0.4667	0.4643		MSE	0.5175	0.6765	0.4438	0.4782	0.4387	0.4743		MSE	0.5166	0.6763	0.4036	0.4291	0.3615	0.3776
		MAPE	30.86	34.01	30.78	31.26	31.45	30.54		MAPE	33.04	34.61	28.57	28.73	38.45	34.25		MAPE	52.63	48.55	43.39	44.82	42.93	36.87
Zhangye	January	β	0.2000	0.2000	7.1×10^{-18}	2.8×10^{-17}	4.4×10^{-18}	3.3×10^{-17}	February	β	0.2000	0.2000	0.0015	5.1×10^{-17}	5.2×10^{-4}	2.1×10^{-17}	March	β	0.2000	0.2000	7.7×10^{-18}	1.2×10^{-17}	1.9×10^{-16}	3.4×10^{-17}
		MSE	0.6117	0.7767	0.4878	0.4922	0.4124	0.4065		MSE	0.8385	1.1600	0.6144	0.6111	0.5121	0.5141		MSE	1.0451	1.3696	0.7658	0.7405	0.6046	0.5914
		MAPE	40.15	47.76	38.60	36.17	35.94	35.40		MAPE	36.11	39.83	29.82	29.05	25.76	26.28		MAPE	28.33	31.43	24.82	25.93	28.67	30.11
	April	β	0.2000	0.2000	0.0161	1.7×10^{-17}	0.0173	2.5×10^{-17}	May	β	0.2000	0.2000	1.7×10^{-18}	1.9×10^{-17}	1.8×10^{-16}	3.9×10^{-18}	June	β	0.2000	0.2000	1.3×10^{-15}	2.9×10^{-18}	0.0127	0.0072
		MSE	1.3259	1.7370	1.0168	1.0110	0.8257	0.8175		MSE	1.1900	1.6304	0.9735	0.8817	0.7552	0.7018		MSE	0.7296	1.0165	0.5744	0.5930	0.4873	0.5133
		MAPE	36.76	41.62	28.62	31.63	28.97	30.41		MAPE	39.46	38.61	31.68	27.79	30.74	28.22		MAPE	35.26	45.10	28.27	28.64	27.10	25.05
	July	β	0.2000	0.2000	5.4×10^{-17}	1.2×10^{-17}	8.6×10^{-18}	1.3×10^{-17}	August	β	0.2000	0.2000	0.0052	3.4×10^{-17}	0.0052	1.0×10^{-17}	September	β	0.2000	0.2000	0.0305	1.8×10^{-17}	0.0141	1.3×10^{-17}
		MSE	0.7510	0.9877	0.6106	0.6152	0.5361	0.5421		MSE	0.9724	1.3537	0.7997	0.7723	0.6561	0.6429		MSE	0.6183	0.7778	0.4645	0.3840	0.3545	0.3001
		MAPE	33.48	40.93	38.22	42.41	36.34	38.98		MAPE	24.29	28.64	21.45	27.53	25.39	36.96		MAPE	20.65	24.56	21.19	24.86	17.27	19.77
	October	β	0.2000	0.2000	0.0013	3.4×10^{-18}	0.0020	1.7×10^{-17}	November	β	0.2000	0.2000	4.0×10^{-17}	3.7×10^{-17}	2.2×10^{-16}	8.7×10^{-18}	December	β	0.2000	0.2000	2.0×10^{-16}	8.7×10^{-18}	3.3×10^{-4}	4.4×10^{-17}
		MSE	0.5372	0.7018	0.3774	0.3794	0.3241	0.3242		MSE	0.6136	0.7163	0.4505	0.4387	0.3500	0.3442		MSE	0.6154	0.7543	0.4967	0.4619	0.3859	0.3931
		MAPE	25.51	31.75	22.63	21.89	26.27	26.43		MAPE	32.65	38.84	26.93	30.92	30.91	32.58		MAPE	35.35	41.16	31.36	30.44	38.45	50.48

Table 3
The decreased RE values relative to FAC model of each month in year 2006.

Month	FAC	SAC	PFAC	PSAC	SPFAC	SPSAC	FAC	SAC	PFAC	PSAC	SPFAC	SPSAC
	Jiuquan						*Mazongshan*					
January	0	−34.50	12.67	10.25	12.67	10.88	0	−25.50	19.77	12.35	36.66	27.95
February	0	−30.81	21.53	23.11	39.35	38.96	0	−42.18	19.14	22.44	32.39	37.62
March	0	−30.43	27.95	24.16	41.45	43.74	0	−31.72	19.02	22.31	30.61	32.55
April	0	−31.17	27.05	28.20	39.47	40.73	0	−21.92	20.34	22.67	32.73	33.22
May	0	−34.91	14.93	23.72	34.81	39.36	0	−12.92	20.34	22.67	32.73	33.22
June	0	−39.25	25.79	24.96	36.58	37.36	0	−36.31	30.46	32.96	45.38	48.65
July	0	−35.72	18.67	19.58	20.42	22.50	0	−36.60	18.25	20.68	24.68	28.15
August	0	−25.08	15.07	12.52	12.54	13.61	0	−17.34	20.11	19.70	28.82	28.58
September	0	−29.92	23.64	22.25	20.85	15.76	0	−29.42	26.84	30.42	32.94	34.92
October	0	−41.28	15.15	12.77	34.20	33.97	0	−25.52	23.27	25.78	17.27	21.33
November	0	−39.03	14.86	10.64	28.98	25.62	0	−17.77	13.72	14.51	28.71	31.28
December	0	−28.40	5.32	1.67	11.00	5.99	0	−28.48	3.56	0.68	7.14	−9.81
Ave.	0	−33.37	18.55	17.82	27.69	27.37	0	−27.13	19.03	20.13	28.73	28.76
	Wuwei						*Zhangye*					
January	0	−28.82	19.74	18.67	24.68	23.86	0	−26.97	20.26	19.54	32.58	33.55
February	0	−26.28	15.29	16.85	22.96	23.04	0	−38.34	26.73	27.12	38.93	38.69
March	0	−42.15	29.79	26.93	39.89	37.37	0	−31.05	26.72	29.15	42.15	43.41
April	0	−44.59	24.09	22.22	38.07	34.24	0	−31.01	23.31	23.75	37.73	38.34
May	0	−34.62	21.04	17.13	28.33	22.15	0	−37.01	18.19	25.91	36.54	41.03
June	0	−27.45	27.62	17.58	29.56	18.78	0	−39.32	21.27	18.72	33.21	29.65
July	0	−30.87	20.80	18.55	33.00	30.59	0	−31.52	18.70	18.08	28.62	27.82
August	0	−37.24	25.88	20.83	33.82	28.06	0	−39.21	17.76	20.58	32.53	33.89
September	0	−29.51	26.07	25.49	29.71	31.53	0	−25.80	24.87	37.89	42.67	51.46
October	0	−24.42	15.90	16.35	13.20	13.65	0	−30.64	29.75	29.37	39.67	39.65
November	0	−30.72	14.24	7.59	15.23	8.35	0	−16.73	26.58	28.50	42.96	43.90
December	0	−30.91	21.87	16.94	30.02	26.91	0	−22.57	19.29	24.94	37.29	36.12
Ave.	0	−32.30	21.86	18.76	28.21	24.88	0	−30.85	22.79	25.30	37.07	38.13

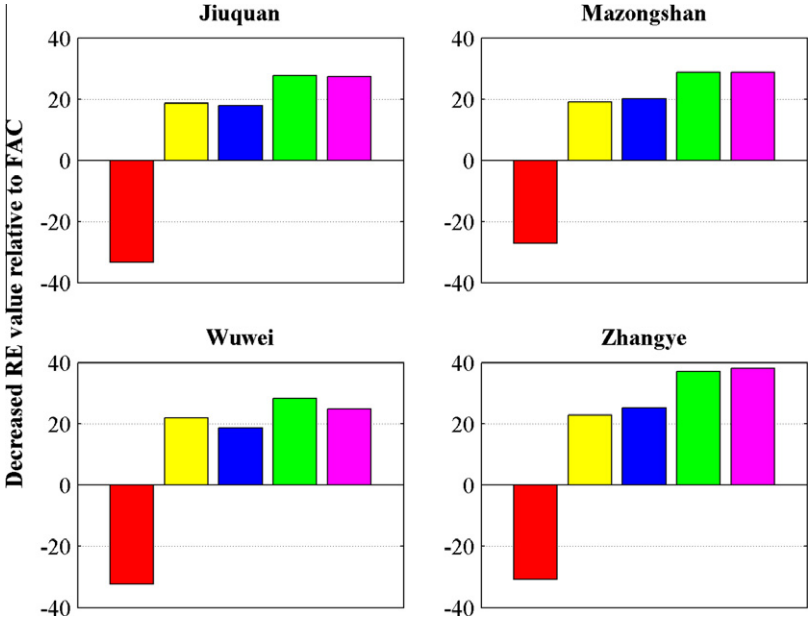

Fig. 7. Decreased RE values of the other five models relative to FAC.

The total sampling period is 6 years, from 2001 to 2006. The wind speed data samples from these four observation sites are presented in Fig. 6.

As seen in Fig. 6, the wind speed data display certain seasonal trends on a yearly cycle. Therefore, it is feasible to forecast future wind speed data using historical data.

3.2. Error evaluation criteria and simulation results

As described in Section 2.4, four modified models are developed. To assess these models, two error evaluation criteria are used: MSE (Mean Square Error) and MAPE (Mean Absolute Percentage Error). They are calculated as follows:

$$\mathrm{MSE} = \frac{1}{n}\sum_{k=1}^{n}\left(x^{(0)}(k) - \hat{x}^{(0)}(k)\right)^2, \tag{16}$$

$$\mathrm{MAPE} = \frac{1}{n}\sum_{i=1}^{n}\left|\frac{x^{(0)}(k) - \hat{x}^{(0)}(k)}{x^{(0)}(k)}\right| \times 100\%, \tag{17}$$

where $x^{(0)} = (x^{(0)}(1), x^{(0)}(2), \ldots, x^{(0)}(n))$ and $\hat{x}^{(0)} = (\hat{x}^{(0)}(1), \hat{x}^{(0)}(2), \ldots, \hat{x}^{(0)}(n))$ represent the actual value and the forecasted value, respectively, and $x^{(0)}(k)$ and $\hat{x}^{(0)}(k)$ represent their kth components.

Table 4
MAPE of the four sites in year 2006.

Site	MAPE (%)					
	FAC	SAC	PFAC	PSAC	SPFAC	SPSAC
Jiuquan	33.1108	37.0450	27.7083	29.2508	31.2275	31.7942
Mazongshan	36.3583	40.1742	33.9808	32.7600	35.0142	32.8758
Wuwei	35.7408	39.8025	31.8292	30.6283	33.3508	31.8533
Zhangye	32.3333	37.5192	28.6325	29.7717	29.3175	31.7225

Because the actual wind speed data values are sometimes equal to 0, the fitness function in PSO cannot choose the MAPE criterion because the process of selecting the most suitable parameters will fail when this is the case. Therefore, the MSE criterion is adopted as the fitness function to update the positions and velocities of the particles. Although MAPE is not appropriate to use as the fitness function in the PSO method, it can be adopted to evaluate the final forecasting performance if the wind speed values are greater than 0. Generally, seasonal trends may exist in yearly cycles for daily average wind speed values. Therefore, we use the daily average wind speed data of 1 month for a period of 5 years (2001–2005) to forecast the wind speed of the same month in 2006 for the four observation sites. It is worth noting that the number of data points in February of 2004 is 29, one greater than for the same month in other years; thus, we only use the first 28. The simulation results for the four wind farm sites are listed in Table 2.

As shown in Table 2, a large number of MSE and MAPE values obtained through the combined strategies are smaller than those obtained by the original FAC and SAC models in the same month. Accordingly, the decreased relative error (RE) of MSE obtained by each model relative to FAC at time t is calculated according to

$$\mathrm{RE}(t,i)=\frac{\mathrm{MSE}_{reference\ model}(t)-\mathrm{MSE}_{model\ i}(t)}{\mathrm{MSE}_{reference\ model}(t)}, \tag{18}$$

where the reference model in our simulation is FAC, model $i(i=1,2,\ldots,6)$ represents one of our six models and $t(t=1,2,\ldots 12)$ stands for one of the 12 months. The resulting RE values are listed in Table 3. In addition, to provide a comprehensive evaluation of the performances of these six models, the Average (Ave.) error criterion is introduced, which is calculated by

$$\mathrm{Ave.}(i)=\sum_{t=1}^{12}\mathrm{RE}(t,i). \tag{19}$$

As seen, the decreased RE values of FAC are necessarily equal to 0. Thus, only the decreased RE values of the other five models relative to FAC are shown in Fig. 7 for the four sites. As shown in Table 3 and Fig. 7, the decreased RE values of SAC relative to FAC at the four sites are all negative, while for the four modified models, all the decreased RE values are positive. This finding implies that all of the MSE values obtained by these four models are smaller than those attained by the original, unimproved FAC and SAC models; it also demonstrates that higher-order models can sometimes, but not always, achieve better performance. Additionally, among these six models, SPFAC and SPSAC obtain smaller prediction errors than other models. Specifically, for the Jiuquan and Wuwei sites, the performance of SPFAC is the best, while for Mazongshan and Zhangye, SPSAC performs better than SPFAC.

The effectiveness of the four modified models relative to the original unimproved FAC and SAC is further supported by the MAPE values for the entire year listed in Table 4.

In contrast to the conclusion drawn from the MSE evaluation criterion, PFAC obtains the most satisfactory results for the Jiuquan site, while PSAC is second best; for Mazongshan, PSAC outperforms the other five models; the best modified model for Wuwei is PSAC; and PFAC produces the most accurate forecasting results for the Zhangye site. Therefore, not one of the four modified approaches is always the best. Preferred models should be selected according to the error evaluation criteria and according to the characteristics of the specific situation at the wind speed observation site. This conclusion agrees with the one attained by Moghram and Rahman [24], who made use of five approaches to forecast the hourly load of a southeastern utility in summer and winter. The best models over summer and winter months were shown to differ, thus it was suggested that approaches should be applied according to the specific appropriate conditions.

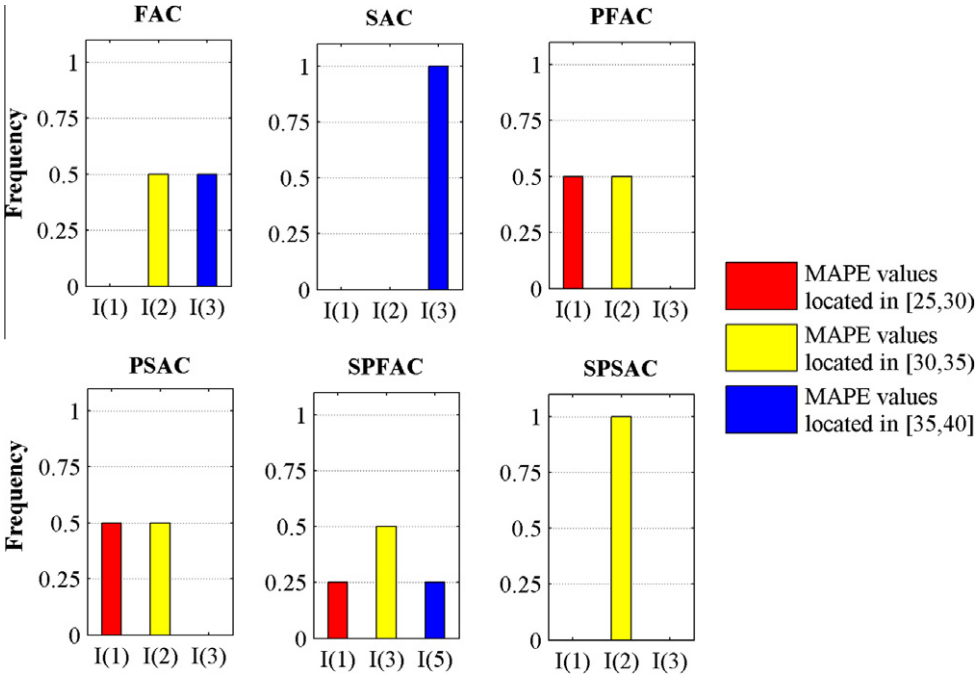

Fig. 8. The frequency histogram of MAPE values obtained by the original and modified models.

The MAPE error for wind speed prediction varies from approximately 25–40% [25], which depends on the forecasting method and wind speed characteristics. Generally, the prediction accuracy increases when the prediction horizon and the data variation decrease [20]. To assess the performance of the combined strategies and the four modified models further, we divide the interval [25] into three intervals of equal length: [25,30), [30,35) and [35,40] and abbreviate them as interval $I(1)$, $I(2)$ and $I(3)$, respectively. Then, the frequencies of the MAPE values obtained by each model for each interval are calculated and are presented in Fig. 8.

By inspecting Fig. 8, it is seen that the modified models have provided satisfactory forecasts. Specifically, all of the MAPE values obtained for PFAC, PSAC and SPSAC are less than 35%, which are much improved compared with the original FAC and SAC models.

4. Conclusions

Knowledge of how to estimate wind speed is quite useful for wind turbine operation and efficient energy harvesting. In this study, on the basis of parameter selection and data decomposition, two combined strategies and four modified models based on FAC and SAC are proposed for wind speed forecasting. Several error evaluation criteria such as the MSE, MAPE and RE are calculated to assess the performance of the developed models. It is shown by the simulation results that the approaches derived from the combined strategies obtain higher prediction accuracy than the FAC and SAC models at the four sampled sites. Thus, suitable parameter selection and data decomposition are excellent ways to improve forecasting accuracy. Moreover, the choice of preferred model changes with different error evaluation metrics and changes in observation site. Therefore, models should be selected according to specific data characteristics. These findings could be significant for research related to wind speed forecasting and will motivate follow-up studies in the future.

Acknowledgements

The work was supported by the National Basic Research Program of China '973' Program (Grant No. 2012CB956200) and the National Natural Science Foundation of China (Grant No. 71171102).

References

[1] Akpinar S, Akpinar EK. Estimation of wind energy potential using finite mixture distribution models. Energy Convers Manage 2009;50:877–84.
[2] van Wijk AJM, Coelingh JP. Wind power potential in the OECD countries, December 1993. Report commissioned by the Energy Research Center, The Netherlands (ECN); 1993.
[3] Torres J, Garcia A, Deblas M, Defrancisco A. Forecast of hourly average wind speed with Arma models in Navarre (Spain). Sol Energy 2005;79(1):65–77.
[4] Erasmo C, Wilfrido R. Wind speed forecasting in the south coast of Oaxaca, Mexico. Renew Energy 2007;32(12):2116–28.
[5] Li G, Shi J. On comparing three artificial neural networks for wind speed forecasting. Appl Energy 2010;87:2313–20.
[6] Ioannis GD, Minas CA, John BT, Petros SD. A fuzzy model for wind speed prediction and power generation in wind parks using spatial correlation. IEEE Trans Energy Convers 2004:19.
[7] Zhou JY, Shi J, Li G. Fine tuning support vector machines for short-term wind speed forecasting. Energy Convers Manage 2011;52:1990–8.
[8] Morales JM, Minguez R, Conejo AJ. A methodology to generate statistically dependent wind speed scenarios. Appl Energy 2010;87(3):843–55.
[9] Monfared M, Rastegar H, Kojabadi HM. A new strategy for wind speed forecasting using artificial intelligent methods. Renew Energy 2009;34:845–8.
[10] Li G, Shi J, Zhou JY. Bayesian adaptive combination of short-term wind speed forecasts from neural network models. Renew Energy 2011;36:352–9.
[11] Cadenas E, Rivera W. Wind speed forecasting in three different regions of Mexico, using a hybrid ARIMA-ANN model. Renew Energy 2010;35:2732–8.
[12] Sancho SS, Angel MPB, Emilio GOG, Antonio PF, Luis P, Daniel P. Hybridizing the fifth generation mesoscale model with artificial neural networks for short-term wind speed prediction. Renew Energy 2009;34:1451–7.
[13] Rajesh GK, Krithika S. Day-ahead wind speed forecasting using f-ARIMA models. Renew Energy 2009;34:1388–93.
[14] Fan CX, Liu SQ. Wind speed forecasting method: gray related weighted combination with revised parameter. Energy Procedia 2011;5:550–4.
[15] Sancho SS, Emilio GOG, Angel MPB, Antonio PF, Luis P. Short term wind speed prediction based on evolutionary support vector regression algorithms. Expert Syst Appl 2011;38:4052–7.
[16] Colorado D, Hernández JA, Rivera W, Martínez H, Juárez D. Optimal operation conditions for a single-stage heat transformer by means of an artificial neural network inverse. Appl Energy 2011;88:1281–90.
[17] Louka P, Galanis G, Siebert N, Kariniotakis G, Katsafados P, Pytharoulis I, et al. Improvements in wind speed forecasts for wind power prediction purposes using Kalman filtering. J Wind Eng Ind Aerodyn 2008;96:2348–62.
[18] Sancho SS, Angel MPB, Emilio GOG, Antonio PF, Luis P, Francisco C. Accurate short-term wind speed prediction by exploiting diversity in input data using banks of artificial neural networks. Neurocomputing 2009;72:1336–41.
[19] Fadare DA. The application of artificial neural networks to mapping of wind speed profile for energy application in Nigeria. Appl Energy 2010;87:934–42.
[20] Guo ZH, Wu J, Lu HY, Wang JZ. A case study on a hybrid wind speed forecasting method using BP neural network. Knowl Based Syst 2011;24:1048–56.
[21] Wang B, Tai NL, Zhai HQ, Ye J, Zhu JD, Qi LB. A new ARMAX model based on evolutionary algorithm and particle swarm optimization for short-term load forecasting. Electr Power Syst Res 2008;78:1679–85.
[22] Leandro DSC, Viviana CM. A novel chaotic particle swarm optimization approach using Hénon map and implicit filtering local search for economic load dispatch. Chaos Solitions Fract 2009;39:510–8.
[23] Guo ZH, Zhao J, Zhang WY, Wang JZ. A corrected hybrid approach for wind speed prediction in Hexi Corridor of China. Energy 2011;36:1668–79.
[24] Elvira LN. Annual electrical peak load forecasting methods with measures of prediction error. Diss Abstr Int 62 Section: B, 2002, 4719.
[25] Yang X, Xiao Y, Chen S. Wind speed and generated power forecasting in wind farm. Zhongguo Dianji Gongcheng Xuebao/Proc Chin Soc Electr Eng 2005;25:1–5 (in Chinese).